Telomerase and poly(ADP-ribose) polymerase-1 activity sensing based on high fluorescence selectivity and sensitivity of TOTO-1 towards G bases in single strand DNA and poly(ADP-ribose)

Haitang Yang [a], Fangjia Fu[b], Wei Li[b], Wei Wei [a]*, Yuanjian Zhang [a], Songqin Liu [a]*

[a] Jiangsu Engineering Laboratory of Smart Carbon-Rich Materials and Device, Jiangsu Province Hi-Tech Key Laboratory for Bio-medical Research, School of Chemistry and Chemical Engineering, Southeast University, Nanjing, 211189, China
[b] Institution of Theoretical and Computational Chemistry, School of Chemistry and Chemical Engineering, Nanjing University, Nanjing 210023, P. R. China

*Corresponding author. Tel.: 86-25-52090613; Fax: 86-25-52090618.
E-mail address: weiw@seu.edu.cn (W. Wei)
liusq@seu.edu.cn (SQ. Liu)

Table of Contents

Experimental Procedures

Reagents

The oligonucleotides used in this paper were synthesized by Shanghai Sangon Biological Engineering Technology & Services Co. Ltd. (Shanghai, China). The sequences were listed in Table S1. TOTO-1 was obtained from Thermo Fisher Scientific (Massachusetts, USA). Nicotinamide adenine dinucleotide (NAD^+) was obtained from Aladdin Reagent Co., Ltd. (Shanghai, China). Rucaparid phosphate (AG014699) was received from MedChemExpress (New Jersey, USA). Human PARP-1 (113kD) was obtained from Trevigen (Gaithersburg, MD, USA). Ultrapure water (18.2 MΩ cm at 25 °C, Barnstead, Thermo Scientific, USA) was used throughout the study.

Real urine samples from normal, inflammation, and bladder cancer patients were received from Nanjing General Hospital of the Chinese People's Liberation Army. The buffer solutions employed in this study were as follows: TS primer DNA hybridization buffer solution (10 mM Tris-HCl, 50 mM NaCl, 1 mM EDTA, pH 7.4); Telomerase extension reaction buffer (20 mM Tris-HCl, pH 8.3, 1.5 mM $MgCl_2$, 1 mM EGTA, 0.63 mM KCl, 0.005% (v/v) Tween 20, 1 mM dNTPs). PARP-1 reaction buffer (R-buffer) (50 mM Tris-HCl, pH 7.4, 50 mM KCl, 2 mM $MgCl_2$, and 50 μM $Zn(OAc)_2$).

Instrument

The fluorescence studies were conducted on a fluorescence spectrometer (Fluoromax-4, Horiba Jobin Yvon, Japan). A quartz cuvette QS 2 mm was used as a sample container. The fluorescence emission spectra were recorded from 503 to 700 nm with a 488 nm excitation wavelength with a 5 nm for the spectral bandwidth for both excitation and emission monochromators. The excitation wavelength was set to 488 nm. The photons from TOTO-1 were collected on Confocal Laser Scanning Microscope (FV3000, Olympus, Japan). The TOTO-labeled DNA products were kept equilibrium and 20 μL of the solution was pipetted onto the prewashed coverslide for imaging.

Cell Culture and Telomerase Extraction.

Telomerase was extracted using the CHAPS method.[1,2] Before telomerase extraction, HeLa cells, A549 cells, and MCF-7 cells were seeded in DMEM supplemented with 10% FBS, penicillin (100 μg/mL), and streptomycin (100 μg/mL) in 5% CO_2, 37 °C incubator. Three kinds of cells were collected in the exponential phase of growth, and the number of cells was calculated by flow cytometry. Then 1 million cells were dispensed in a 1.5 mL eppendorf tube, washed twice with ice-cold PBS solution by centrifugation at 1800 rpm for 5 min, After discarding the supernatant carefully, the cells were redispersed in 200 μL of ice-cold CHAPS lysis buffer. The cells were incubated for 30 min on ice and then centrifuged for 20 min (12 000 rpm, 4 °C). Finally, the cleared lysate which contained cell extracts corresponding to 5000 cells per μL, was carefully transferred to a fresh tube, flash frozen, and stored at −80 °C before use.

Optimization of the detection conditions

To achieve the best performance, the concentrations of TS primer, ds DNA, TOTO-1, Exo III and the incubation time for telomerase detection were tested. When the concentration of TS primer increased to 4 μM, the peak current of TOTO-1 leveled off (Figure S7A). And when the concentration of TOTO-1 increased to 200 nM, a fluorescence plateau was obtained (Figure S7B). Concentration of Exo III and incubated time were also optimized. As shown in Figure S7C, it can be observed that the background signal decreased with the increasing concentration of Exo III and incubation time (Figure S7D). So, 1 U/μL Exo III was selected and 120 min were the optimal time for Exo III incubation. Similarly, the optimized condition for PARP-1 detection was 150 nM dsDNA, the optimal time for both PARP-1 incubation and catalysis were 60 min. To obtain the reduced the background noise, 1 U/μL Exo III was selected and 120 min were the optimal time for Exo III incubation (Figure S8).

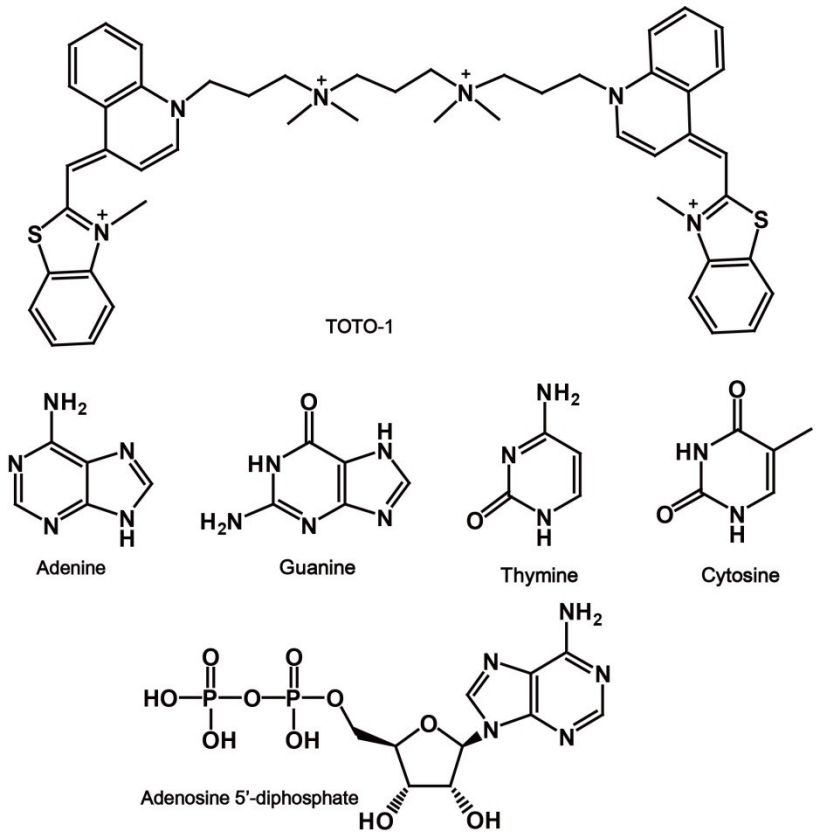

Figure S1. The chemical structure of TOTO-1 and nucleotide bases.

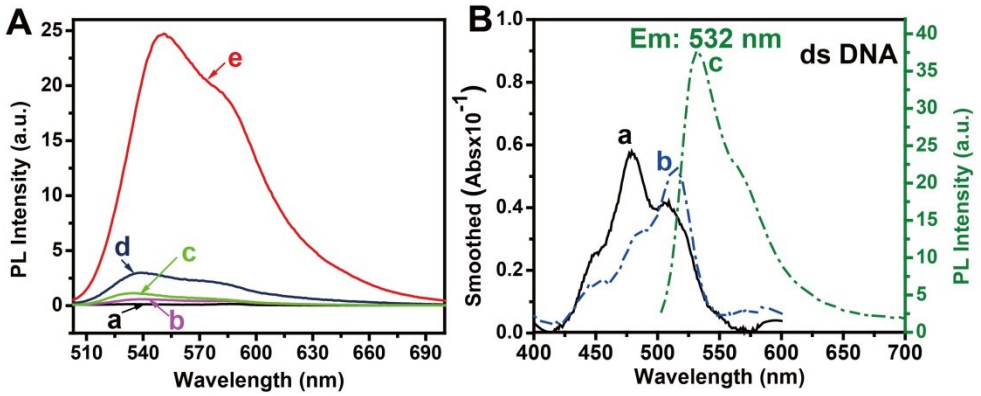

Figure S2. (A) Photoluminence (PL) spectra of 250 nM TOTO-1 in the presence of 86 nM Poly(dG), poly(dA), poly(dT) and poly(dC). a: TOTO-1, b: poly(dT)-TOTO-1, c: poly(dC)-TOTO-1, d: Poly(dA)-TOTO-1, e: Poly(dG)-TOTO-1. (B) Absorption of free TOTO-1 (a) and dsDNA-TOTO-1 (b) and PL of dsDNA-TOTO-1.

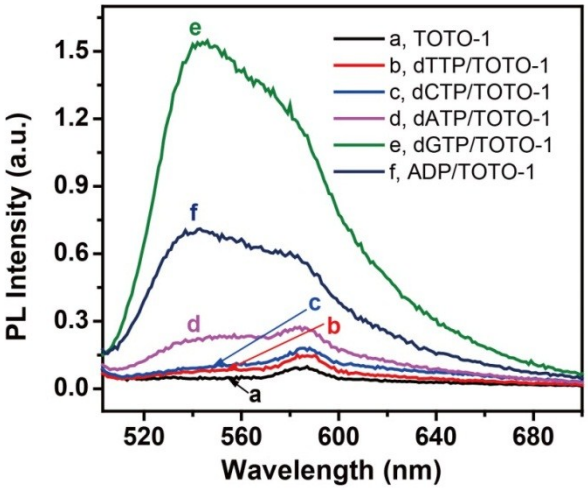

Figure S3. Fluorescence spectra of TOTO-1 in the presence of dGTP, dATP, dCTP, dATP and ADP.

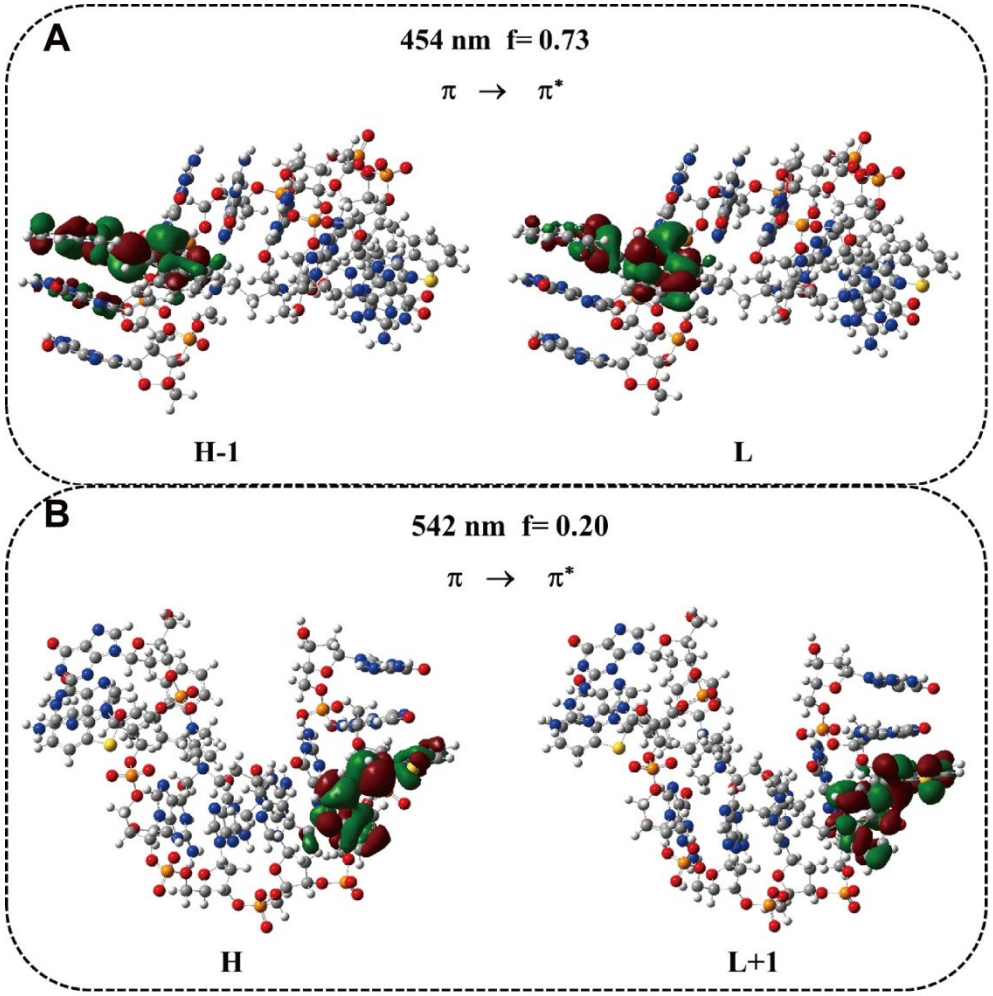

Figure S4.The orbital distribution of excited states transition for TOTO-1/ Poly(dG).

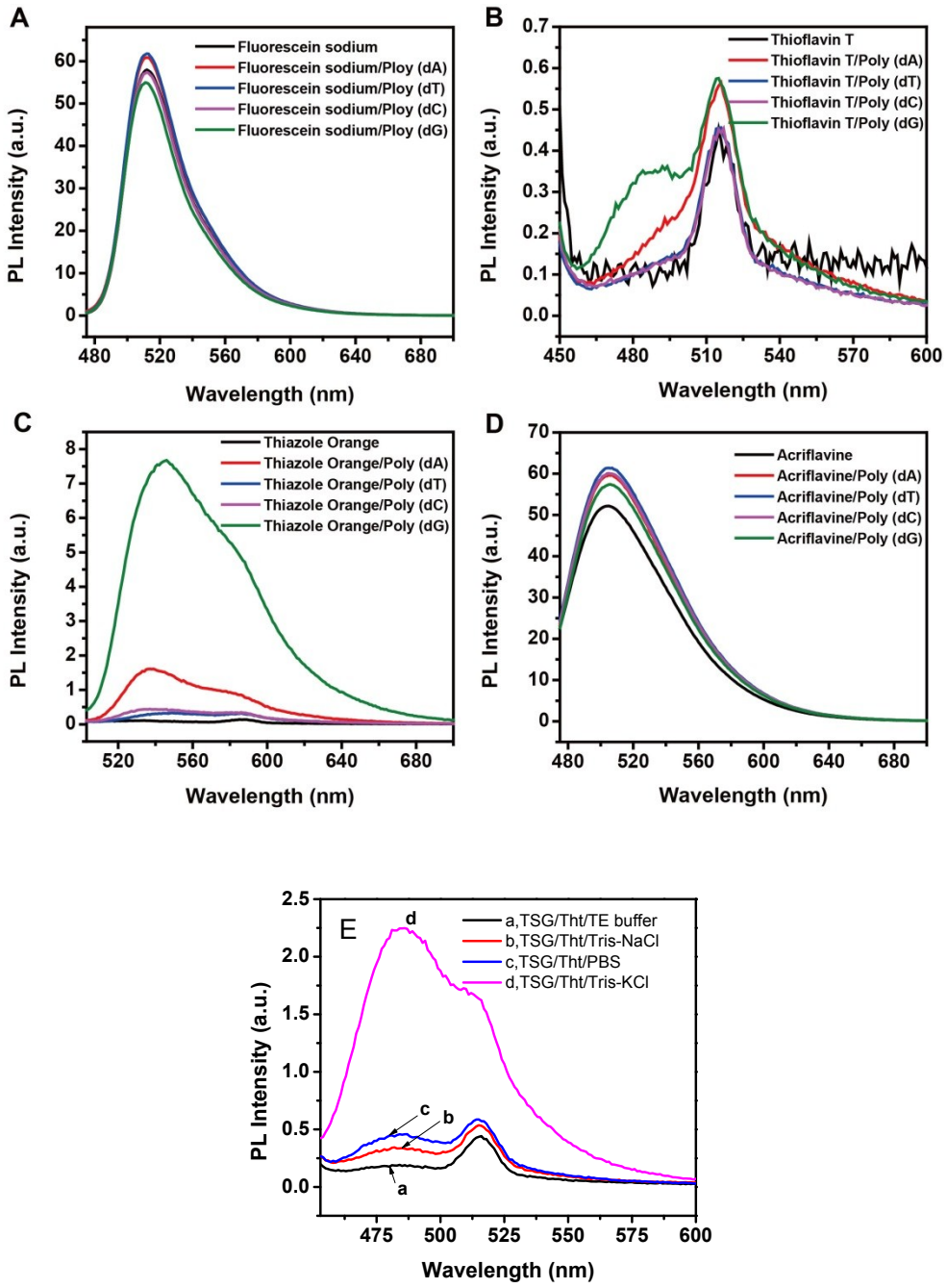

Figure S5. PL spectra of fluorescein sodium(A), thioflavine T(B), thiazole orange(C), acriflavine (D) and fluorescein sodium(A), thioflavine T(B), thiazole orange(C), acriflavine (D) with poly(dA), poly(dT), poly(dC) and poly(dG) at the concentration of 86 nM. (E) PL spectra of G-quadruplex indicator thioflavine T (Tht) with the standard $(TTAGGG)_8$ sequences in different buffers. It proved that G-quadruplex didn't formed in the PBS.

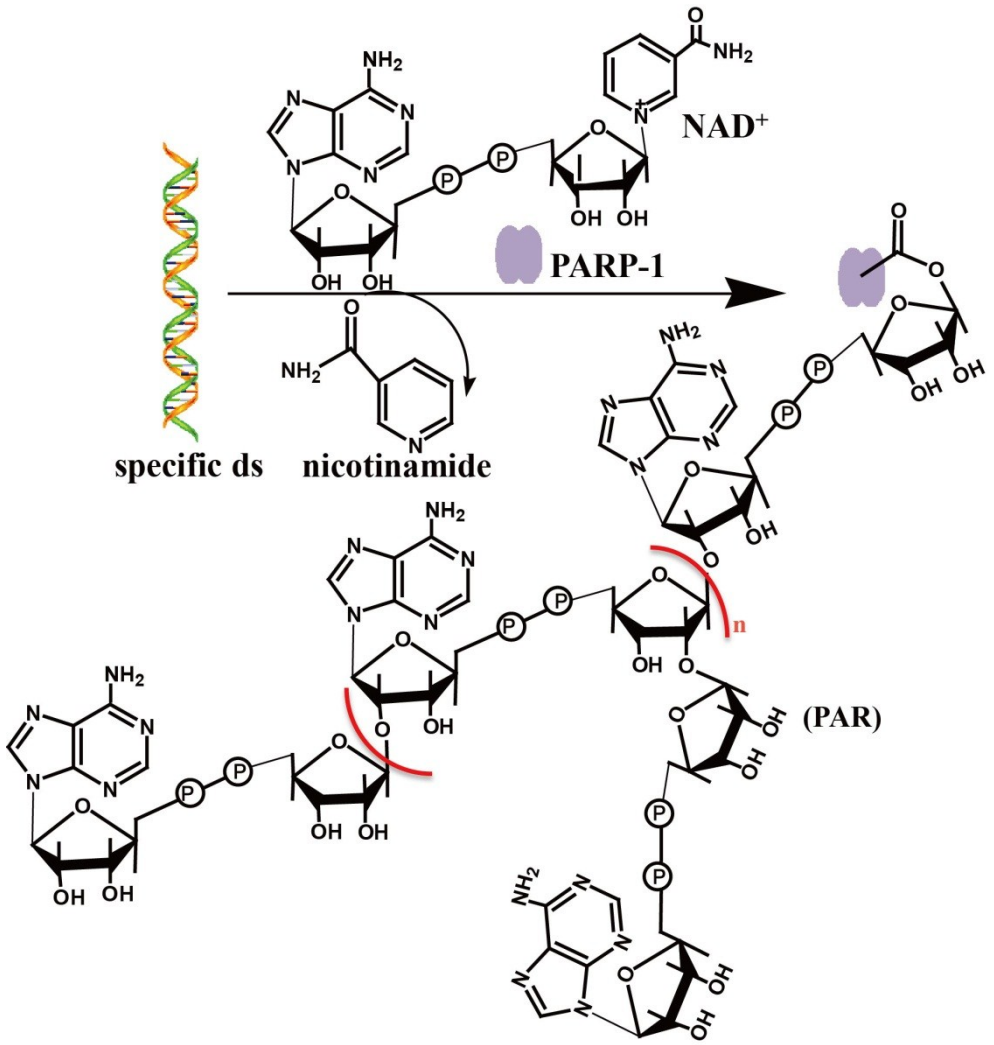

Figure S6. Schematic illustration of the production of PAR catalyzed by PARP-1.

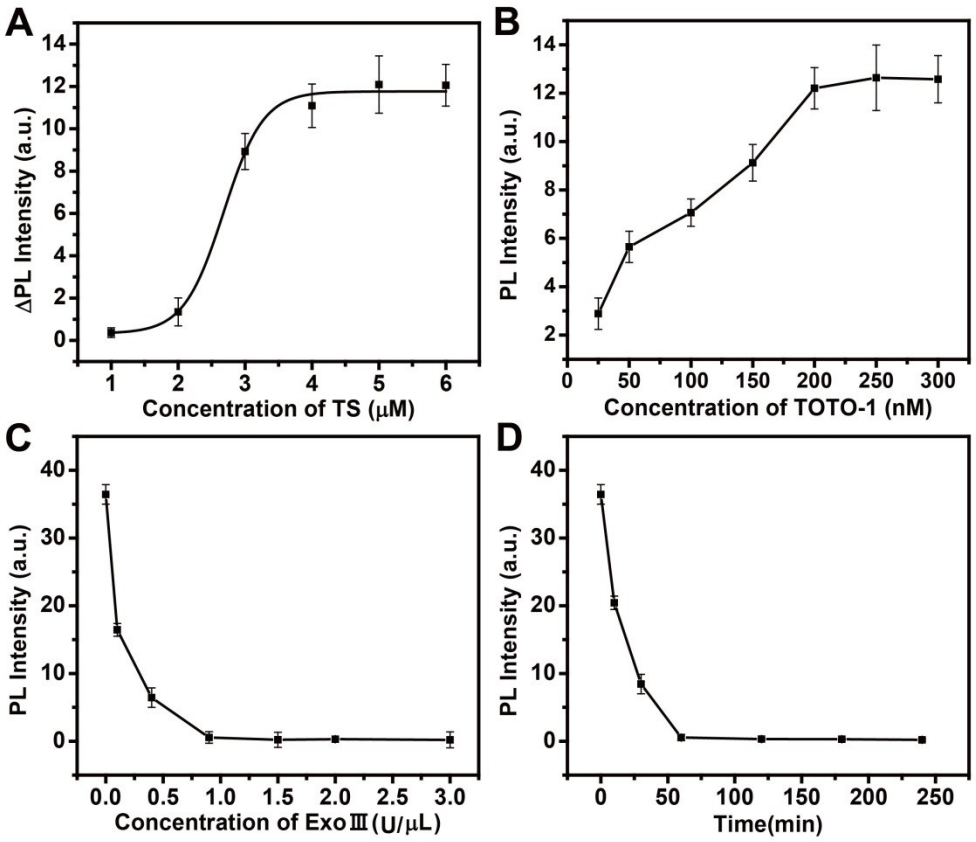

Figure S7.The optimization of the concentrations of TS primer (A), TOTO-1(B), Exo III (C) and the incubation time of Exo III (D).

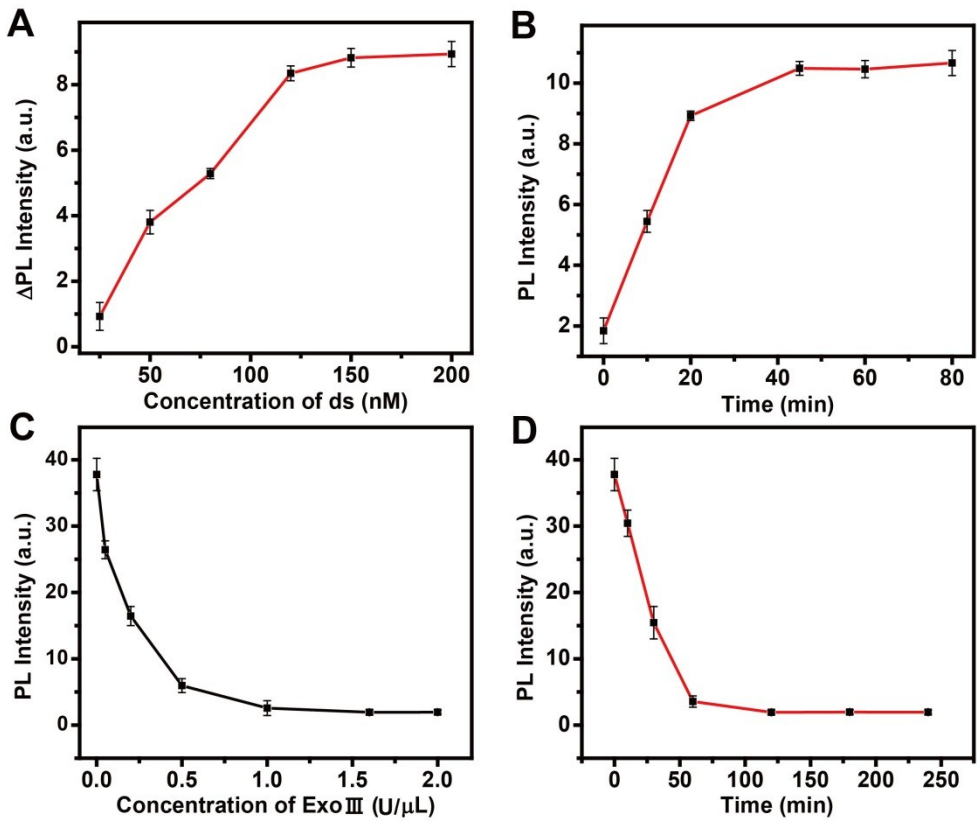

Figure S8. The optimization of the concentrations of specific ds DNA (A), incubation time of 1.0 U PARP-1 (B), the concentrations of Exo III (C) and incubation time of Exo III (D).

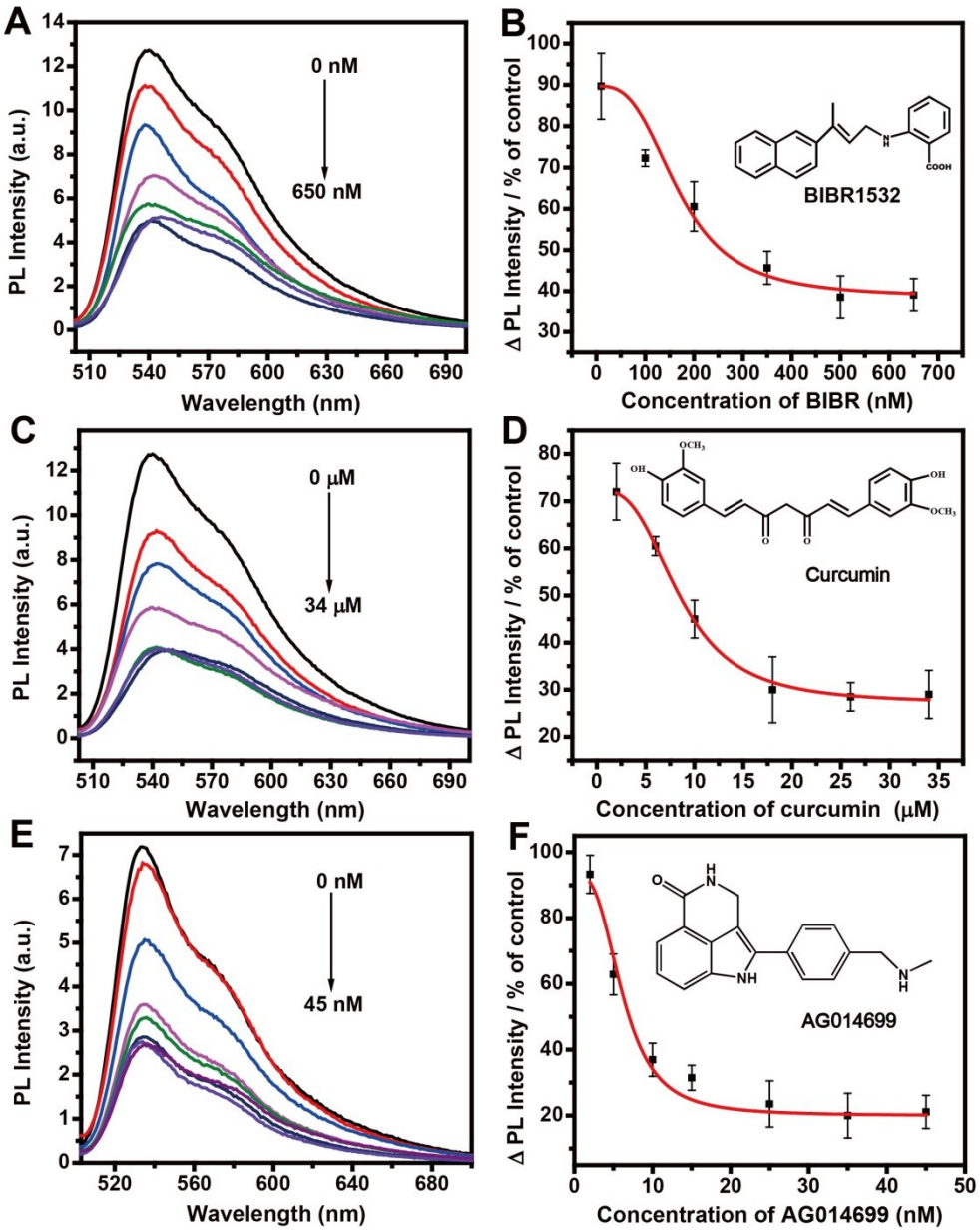

Figure S9. PL spectra of the samples with increasing concentrations inhibition effect of BIBR 1532(A) and curcumin (C) on telomerase activity of inhibitors. The inhibition effects of BIBR 1532(B) and curcumin (D) on telomerase activity. 750 A549 cells/mL was used. (E) PL spectra of the samples with increasing concentrations inhibition effect of AG014699 on PARP-1. (F) The inhibition effect of AG014699 on PARP-1 activity. 0.8 U PARP-1 was used. Error bars showed the standard deviation of three experiments.

Table S1. Sequences of the Oligonucleotides Used in the Experiments.

Name	Sequence
TS primer	5′-AATCCGTCGAGCAGAGTT-3′
cDNA	5′-AACTCTGCTCGACGGATT-3′
Active ssDNA1	5’-CCCGTGCGTGCGCGAGTGAGTTG-3’
Active ssDNA2	5’-CAACTCACTCGCGCACGCACGGG-3’

Table S2. Comparison of Analytical Performance of Various Methods for Determination of PARP-1 Activity.

Method	System	Detection Range	Detection Limit	Reference
UV-vis	ADP-ribose-pNP	semiquantitative	-	3
UV-Vis	AuNRs aggregation based biosensor	0.05 – 1.0 U	0.006 U	4
UV-Vis	AuNPs based biosensor	0.43 - 1.74 nM	0.32 nM	5
UV-Vis	Hemin-graphene based sensors	0.05 – 1 U	0.03 U	6
DPV	PANI	0.005 ~ 1 U	0.002 U	7
SWV	RuHex	0.01 - 1 U	0.003 U	8
Fluorescence	CCP and scGFP	1 - 45 nM	1 nM	9
fluorescence	TOTO-1	0.02-1.5 U	0.02 U (0.04 nM)	this work

Table S3. Detection of PARP-1 in human serum samples, IOSE80 and A2780.[a]

Sample	Added (U)	Found (U)	Recovery (%)	RSD (%, n=3)
Human serum	0.1	0.106	105.9	5.18
	0.2	0.204	102.0	4.97
	0.5	0.491	98.1	3.86
	0.8	0.82	102.5	3.57
IOSE80	0	0.05	-	5.36
	0.1	0.159	109	6.22
	0.2	0.246	98	2.48
	0.5	0.57	104	7.89
A2780	0	0.45	-	6.25
	0.1	0.553	103	7.42
	0.2	0.652	101	8.21
	0.5	0.92	94	7.65

[a]Human serum samples are sampling from healthy donors at the Second Affiliated Hospital of Southeast University, Nanjing, China.

Reference

1 X. Liu, M. Wei, Y. J. Liu, B. J. Lv, W. Wei, Y. J. Zhang, S. Q. Liu, Anal. Chem., 2016, **88**, 8107-8114.

2 Y. J. Liu, M. Wei, X. Liu, W. Wei, H. Y. Zhao, Y. J. Zhang, S. Q. Liu, Chem. Commun., 2016, **52**, 1796-1799

3 A. C. Nottbohm, R. S. Dothager, K. S. Putt, M. T. Hoyt, P. J. Hergenrother, *Angew. Chem. Int. Ed.,* 2007, **46**, 2066-2069.

4 S. Wu, M. Wei, H. Yang, J. Fan, W. Wei, Y. Zhang, S. Liu, *Sens. Actuators B,* 2018, **259,** 565-572.

5 Y. Xu, J. Wang, Y. Cao, G. Li, *Analyst*, 2011, **136**, 2044-2046.

6 Y. Liu, X. Xu, H. Yang, E. Xu, S. Wu, W. Wei, J. Chen, *Analyst*, 2018, **143**, 2501-2507.

7 Y. Liu, J. Fan, L. Shangguan, Y. Liu, Y. Wei, W. Wei, S. Liu, *Talanta*, 2018, **180**, 127-132.

8 Y. Xu, L. Liu, Z. Wang, Z. Dai, *ACS Appl. Mater. Interfaces*, 2016, **8**, 18669-18674.

9 S. Tang, Z. Nie, W. Li, D. Li, Y. Huang, S. Yao, *Chem. Commun.*, 2015, **51**, 14389-14392.